Dzyaloshinskii-Morija interaction and local magnetic anisotropies in U_2Pd_2In: Ground state and metamagnetic transition

L. M. Sandratskii
Max-Planck-Institut für Mikrostrukturphysik, Weinberg 2, 06120 Halle, Germany
(Received 17 June 2016; revised manuscript received 19 September 2016; published 14 November 2016)

U_2Pd_2In is the material where the elements of the geometrical frustration of the lattice coexist with strong spin-orbit coupling (SOC). The ground state of the system is a noncollinear planar magnetic structure with orthogonal atomic magnetic moments. There are three possible physical mechanisms that can lead to this nontrivial magnetic structure: frustrated isotropic exchange interaction, Dzyaloshinskii-Morija interaction (DMI), and magnetic anisotropy. Our first-principles calculations show that in the case where the SOC is neglected, and therefore the DMI and magnetic anisotropy are absent, the ground state structure is the collinear ferromagnetic one. The leading contribution to the stabilization of the magnetically compensated configuration of orthogonal atomic moments is provided by the local magnetic anisotropy of the U moments. A weaker DMI leads to the lifting of the degeneracy between the magnetic states with different local chirality. The established hierarchy of the interactions allows us to explain the metamagnetic phase transition in the in-plane external magnetic field. The analysis of the noncollinearity of the spin and orbital moments of the same U atom appearing in the applied external field show that the trend to the antiparallel orientation of the two atomic moments following from the third Hund's rule is much stronger than the trend to the parallel orientation of the moments due to the applied external magnetic field.

DOI: 10.1103/PhysRevB.94.184414

I. INTRODUCTION

The interplay of effective forces acting on atomic moments in magnetic systems leads to numerous interesting phenomena. For example, the geometric frustration [1] of exchange interactions stimulates the formation of nontrivial noncollinear magnetic structures [2–4]. On the other hand, the competition between isotropic Heisenberg exchange interaction and the consequences of the spin-orbit coupling (SOC)—Dzyaloshinskii-Morija interaction [5,6] (DMI) and magnetic anisotropy—leads to the formation of helical and skyrmionic magnetic structures [7–9]. In noncentrosymmetric atomic structures DMI is responsible for selective chirality of the magnetic configurations [10,11]. The reachness of magnetic configurations increases further if the systems are subjected to the magnetic field. The study of the materials with nontrivial noncollinear magnetic structures is an important task since, on one hand, it deepens our understanding of the fundamental magnetic interactions and, on the other hand, suggests new materials for modern applications.

In this respect, the uranium compound U_2Pd_2In is an interesting material where the possibility of geometrical frustration of the nonferromagnetic interatomic interactions coexists with strong SOC typical for heavy elements. The experiment [12] revealed two remarkable properties of U_2Pd_2In. The first is the formation of a nontrivial planar noncollinear magnetic structure with orthogonal U atomic moments. The second is the metamagnetic first-order phase transition in the external magnetic field applied parallel to the plane of magnetic moments.

The purpose of this paper is to reveal the physical origin of the peculiar ground-state magnetic structure of U_2Pd_2In and to suggest an interpretation of the metamagnetic phase transition. To fulfill this aim we combine (i) first-principles calculations, (ii) the study of the model bilinear Hamiltonian of interacting atomic moments, and (iii) symmetry arguments to disclose the interactions responsible for the magnetism of U_2Pd_2In. The first-principles calculations are performed for various noncollinear magnetic configurations with and without applied magnetic field.

The paper is organized as follows. Section II presents theoretical approach. In Sec. III we discuss the crystal lattice and symmetry operations of magnetic structures in nonrelativistic and relativistic cases. Section IV presents the results of the first-principles calculations for various magnetic configurations. In Sec. V we consider the properties of the model bilinear Hamiltonian of interacting atomic moments. Section VI deals with the results of the calculations for U_2Pd_2In in applied magnetic field.

II. THEORETICAL APPROACH

The main tool of our theoretical study is first-principles calculations within the framework of the density functional theory (DFT) for noncollinear magnetic configurations (see Ref. [13] and references therein). In these calculations, not only the values of the magnetic moments but also their directions are self-consistently determined. This means that if the magnetic structure assumed at the beginning of an iteration does not correspond to a torque-free magnetic state, the instability of the structure will be revealed and the output of the iteration will provide the magnetic configuration that is different from the input one.

The electronic Kohn-Sham Hamiltonian of a noncollinear magnet can be presented in the form

$$H = T + V + H_{so}, \tag{1}$$

where T is the kinetic energy operator, V is two-by-two electronic potential, and H_{so} is the operator of the spin-orbit coupling. Assuming a spherically symmetric form of the atomic potentials the effective potential in ith atomic sphere

can be written in the form

$$V_i(r) = U(\theta_i,\phi_i)^\dagger \begin{pmatrix} V_i^+(r) & 0 \\ 0 & V_i^-(r) \end{pmatrix} U(\theta_i,\phi_i), \qquad (2)$$

where angles θ_i and ϕ_i determine the direction of the atomic spin moment and define the local spin-coordinate system of the ith atom characterized by the diagonal form of the potential matrix; V_i^+ and V_i^- are the spin-up and spin-down potentials in the local system; $U(\theta_i,\phi_i)$ is the matrix of spin-$\frac{1}{2}$ rotation transforming the potential from the atomic system of the ith atom to the global system. The operator of the spin-orbit coupling is taken in the form [14]

$$\mathbf{H}_{\rm so} = \frac{1}{(2c)^2}\frac{1}{r}\left[\begin{pmatrix} \frac{1}{M_+^2}\frac{dV^+}{dr} & 0 \\ 0 & \frac{1}{M_-^2}\frac{dV^-}{dr} \end{pmatrix}\sigma_z\hat{l}_z + \frac{1}{M_{av}^2}\frac{dV^{av}}{dr_v}(\sigma_x\hat{l}_x + \sigma_y\hat{l}_y)\right], \qquad (3)$$

where

$$V^{av}(r) = \tfrac{1}{2}(V^+(r) + V^-(r)) \qquad (4)$$

and

$$M_\alpha = \frac{1}{2}\left(1 - \frac{1}{c^2}V^\alpha\right), \quad \alpha = av, +, -. \qquad (5)$$

$\sigma_x,\sigma_y,\sigma_z$ are the Pauli matrices and $\hat{l}_x,\hat{l}_y,\hat{l}_z$ are the operators of the components of the orbital momentum. In Eqs. (3) and (5), the Rydberg atomic units are used.

We will refer to the full Hamiltonian of Eq. (1) as relativistic Hamiltonian. The case where the spin-orbit coupling $H_{\rm so}$ is neglected will be referred to as nonrelativistic. We will also perform calculations of U_2Pd_2In in applied magnetic field. The magnetic field enters the Hamiltonian through the Zeeman term acting on both spin and orbital atomic magnetic moments [15].

An important role in the prediction and interpretation of the results of the calculations is played by the symmetry analysis. It is crucial that the symmetry analysis of the nonrelativistic and relativistic Hamiltonians must be performed on the basis of different sets of symmetry operators. In the nonrelativistic problems the adequate set of the operators are the spin-space groups that allow for different transformation of the spin and space subsystems. These operators have the form $\{\alpha_S|\alpha_R|\boldsymbol{\tau}_\alpha + \boldsymbol{R}_n\}$ where the real-space (orbital) part of the operation $\{\alpha_R|\boldsymbol{\tau}_\alpha + \boldsymbol{R}_n\}$ transforms the atomic positions but does not change the directions of the magnetic moments, whereas the spin rotation α_S performs the point transformation of the atomic moments. Here α_R is a real-space point operation, $\boldsymbol{\tau}_\alpha$ is nonprimitive translation corresponding to α_R, and $\boldsymbol{R}_n$ are lattice translations. We will consider only those space operations that transform crystal lattice into itself since the consideration of the displaced lattices does not bring information useful for our purposes. The action of the operation $\{\alpha_S|\alpha_R|\boldsymbol{\tau}_\alpha\}$ on a magnetic crystal is defined as

$$\{\alpha_S|\alpha_R|\boldsymbol{\tau}_\alpha\}\mathbf{S}(\boldsymbol{a}_i + \boldsymbol{R}_n) = \alpha_S\boldsymbol{S}[\{\alpha_R|\boldsymbol{\tau}_\alpha\}^{-1}(\mathbf{a}_i + \mathbf{R}_n)], \qquad (6)$$

where $\mathbf{S}(\boldsymbol{a}_i + \boldsymbol{R}_n)$ gives the vector of atomic moment at the ith atomic position in the nth unit cell. The operations of the spin-space group can be combined with time-reversal operation Θ.

Since the spin-space operations with different α_S and α_R do not preserve the form of the spin-orbit coupling term $H_{\rm so}$, they cannot be applied to the study of the relativistic problems. In the relativistic problems the spin-space group reduces to usual space group where $\alpha_S = \alpha_R$. The difference of the groups of the symmetry operators in the nonrelativistic and relativistic problems results in dramatically different properties of relativistic and nonrelativistic magnetic systems.

The symmetry arguments will be used to study three different types of the properties of the system. First, the symmetry analysis is employed to predict the calculational stability of a *given* magnetic structure. The following principle is used: If the considered magnetic structure is distinguished by symmetry in the sense that any deviation of the atomic moments from the directions specified by the magnetic structure disturbs at least one of the symmetry operations, this magnetic configuration is calculationally stable [13]. The calculational stability does not necessarily mean that the configuration corresponds to the lowest energy state and is *physically* stable. Instead, it signifies the symmetry-determined vanishing of the torque on the atomic moments. Such a calculationally stable state can correspond to an energy maximum or saddle point of the energy considered as a function of the directions of atomic moments. The calculational stability of the state despite its possible physical instability is explained by the absence of random fluctuations within the standard DFT calculations and can be regarded as the consequence of the symmetry constraint [16] imposed on the calculational results by the symmetry of the initial state.

A second type of the symmetry analysis establishes the equivalence of *different* magnetic configurations. If an operation transforms the Hamiltonian of one magnetic structure of the system into the Hamiltonian of another magnetic structure the two magnetic structures are equivalent in the sense that they have equal energies and their wave functions are connected by the same transformation. Obviously, it is sufficient to perform the DFT calculation for one of the equivalent magnetic configurations.

Third, it is a common practice to map the itinerant-electron systems onto a model Hamiltonian of interacting atomic moments that helps to make the physics of the system more transparent. Here the symmetry analysis helps to reduce the number of independent parameters of the effective Hamiltonian. The details of the symmetry analysis of the bilinear Hamiltonian of interacting atomic moments are given in Sec. V A.

III. CRYSTAL LATTICE AND SYMMETRY OPERATIONS

The unit cell of U_2Pd_2In is shown in Fig. 1. The plane of the U moments forms the Shastry-Sutherland-type lattice known as one of the systems with geometrical frustration [17,18]. The topological equivalence [19] of the U plane to the Shastry-Sutherland lattice is demonstrated in Fig. 2. If the exchange interaction between atoms connected by thick red lines in Figs. 2(a) and 2(b) is strong antiferromagnetic the atoms form antiferromagnetic dimers. The exchange interactions between atoms connected by thin blue lines cannot be satisfied that leads to the magnetic frustration.

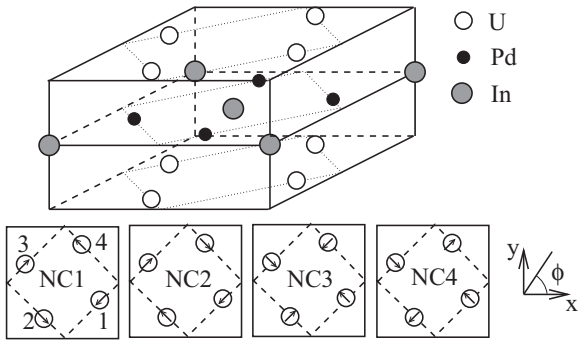

FIG. 1. Unit cell of U_2Pd_2In. Below the four noncollinear magnetic structures used in the analysis of the experiment. In the figure showing the NC1 structure the numbering of the U sublattices accepted in the paper is given.

The symmetry of the atomic lattice is characterized by 16 real-space point operations collected in Table I. The nonmagnetic state of the system is invariant with respect to the time reversal and, therefore, each of the 16 operations can be accompanied by time reversal.

As mentioned above, in the nonrelativistic problems each orbital operation can be combined with arbitrary spin rotation. In the relativistic problems the spin and orbital point transformations must coincide.

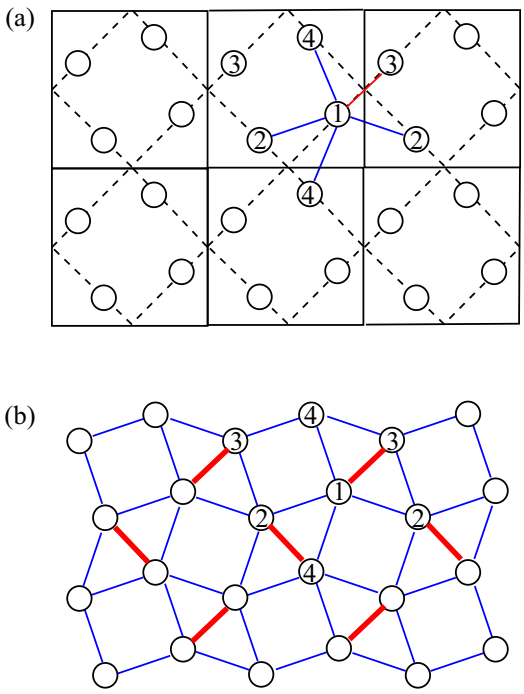

FIG. 2. (a) The fragment of the plane containing U atoms. The solid lines connect the atoms whose interaction is discussed in Sec. V A. (b) The same fragment of the U plane in the form revealing topological equivalence to the Shastry-Sutherland lattice. The Shastry-Sutherland model considers the case of antiferromagnetic exchange interactions between atoms connected by both thick red and thin blue lines. The strong "red" interaction leads to the formation of the antiferromagnetic dimers. The blue antiferromagnetic interactions cannot be satisfied that leads to the frustration.

TABLE I. Symmetry operations of the atomic lattice of U_2Pd_2In. First column: number of the operation. Second column: symbol of the operation. E is the unity operation; $C_{n\alpha}$ are proper rotations by angle $2\pi/n$ about the α axis; $\alpha = x,y,z$ correspond to the x,y,z axes, $\alpha = a$ corresponds to the $y = x$ axis in the $z = 0$ plane, $\alpha = b$ corresponds to the $y = -x$ axis in the $z = 0$ plane; $S^{\pm}_{4z}$ are improper rotations about the z axis by angle $\frac{\pi}{2}$; σ_β is the reflexion in the β plane, $\beta = x,y,z$ correspond to the $x = 0$, $y = 0$, $z = 0$ planes, $\beta = a$ corresponds to the $y = -x$ plane, $\beta = b$ corresponds to the $y = x$ plane. Third column: If nonzero, it gives the vector of nonprimitive translation $\boldsymbol{\tau} = (0.5,0.5,0)$. Forth column: the result of the action of the point operation on axial vector (m_x,m_y,m_z). Fifth column: the positions of the U atoms into which the U_{1-4} atoms are transformed by the operation.

No.	OP	$\boldsymbol{\tau}$	**m**	at. permutation
1	E	0	(m_x,m_y,m_z)	1234
2	C_{2x}	$\boldsymbol{\tau}$	$(m_x,-m_y,-m_z)$	2143
3	C_{2y}	$\boldsymbol{\tau}$	$(-m_x,m_y,-m_z)$	4321
4	C_{2z}	0	$(-m_x,-m_y,m_z)$	3412
5	C_{2b}	$\boldsymbol{\tau}$	$(-m_y,-m_x,-m_z)$	3214
6	C^{-}_{4z}	0	$(m_y,-m_x,m_z)$	2341
7	C^{+}_{4z}	0	$(-m_y,m_x,m_z)$	4123
8	C_{2a}	$\boldsymbol{\tau}$	$(m_y,m_x,-m_z)$	1432
9	I	0	(m_x,m_y,m_z)	3412
10	σ_x	$\boldsymbol{\tau}$	$(m_x,-m_y,-m_z)$	4321
11	σ_y	$\boldsymbol{\tau}$	$(-m_x,m_y,-m_z)$	2143
12	σ_z	0	$(-m_x,-m_y,m_z)$	1234
13	σ_b	$\boldsymbol{\tau}$	$(-m_y,-m_x,-m_z)$	1432
14	S^{+}_{4z}	0	$(m_y,-m_x,m_z)$	4213
15	S^{-}_{4z}	0	$(-m_y,m_x,m_z)$	2341
16	σ_a	$\boldsymbol{\tau}$	$(m_y,m_x,-m_z)$	3214

Below, we consider the results of the first-principles nonrelativistic and relativistic calculations for various magnetic configurations of U_2Pd_2In. Before going over to the discussion of the results of the calculations it is useful to summarize the symmetry-determined properties of collinear ferromagnetic configuration and noncollinear NC1-4 configurations shown in Fig. 1. These noncollinear configurations were used in the analysis of experiment [12].

A. Symmetry properties of magnetic structures of U_2Pd_2In in nonrelativistic calculations

In nonrelativistic problems any collinear configuration is calculationally stable. This stability is governed by the symmetry with respect to the pure spin rotations about the magnetization axis. This symmetry is disturbed if an atomic moment deviates from the magnetization axis. On the other hand, all collinear magnetic structures obtained from the given one by an arbitrary rotation of all atomic moments are equivalent to each other.

Also the four noncollinear magnetic structures NC1-4 with orthogonal atomic moments are calculationally stable. The calculational stability of the NC1 structure follows from the three symmetry operations leaving this structure invariant: (1) operation $\Theta\{\sigma_z|\sigma_z|0\}$ is a symmetry operation of any planar magnetic structure with atomic moments parallel to the $z = 0$

plane, which is responsible for keeping all moments in-plane, (2) operation $\{C_{4z}|C_{4z}|0\}$ performing the rotation by 90° about the z axis keeps the in-plane moments orthogonal to each other, and (3) operation $\Theta\{C_{2a}|C_{2a}|(0.5,0.5,0)\}$ of the 180° rotation about the $x = y$ axis does not allow the moments of atoms U_1 and U_3 to deviate from the [110] direction. Similar arguments are valid for NC2-4 structures.

The four noncollinear structures NC1-4 are equivalent to one another since there are operations transforming them into each other. For example, NC1 is transformed into NC2 by the 180° spin rotation about the $x = y$ axis, into NC4 by the pure spin rotation by 90° about the z axis, and into NC3 by the combination of the above two spin rotations.

B. Symmetry properties of magnetic structures of U_2Pd_2In in relativistic calculations

If the SOC is taken into account, the states NC1-4 remain calculationally stable since the symmetry operations responsible for the symmetry constraint in the nonrelativistic case, considered above, transform in the same way both spin and orbital variables and therefore are applicable also in the relativistic case. The four configurations, however, become inequivalent since the symmetry operations transforming these structures into one another in the nonrelativistic approach act differently on spin and orbital subsystems and are not operative in the relativistic case. As a result, the energies of the four NC1-4 configurations are different (see Sec. IV B below).

The symmetry properties of the FM configurations in the relativistic case differ strongly from those in the nonrelativistic case. First, the ferromagnetic configurations with different directions of the moments with respect to the atomic lattice are now inequivalent. The symmetry reason for the inequivalence is the same as in the case of NC1-4 structures: The pure spin rotations are not allowed in the relativistic problems. The physical origin of this inequivalence is the magnetic anisotropy. Second, in contrast to the nonrelativistic case, the relativistic collinear ferromagnetic configurations are, in general, not calculationally stable. As an example, we consider two in-plane ferromagnetic configurations. First is the configuration with atomic moments parallel to the x axis [Fig. 3(a)]. The symmetry group of this magnetic state contains eight operations: E, C_{2x}, ΘC_{2y}, ΘC_{2z}, I, σ_x, $\Theta\sigma_y$, $\Theta\sigma_z$. Here we give only the point transformations and time reversal. The corresponding nonprimitive translation can be found in Table I. These operations impose the following constraint on the system: Since C_{2x}, C_{2y}, C_{2z} transform atom 1 into, respectively, atoms 2, 4, 3 (see Table I), all U atoms in this configuration are equivalent. These operations also impose symmetry restrictions on the components of the atomic moments: All of them must have equal m_x components and the m_y components satisfying the relations $m_{1y} = -m_{2y} = m_{3y} = -m_{4y}$. Importantly, there is no symmetry constraint of zero m_y components. In the relativistic calculations the initially ferromagnetic moments parallel to the x axis deviate from their parallel directions assuming nonzero m_y components leading to the configuration shown in Fig. 3(a).

In the case of the ferromagnetic moments parallel to the [110] direction [see Fig. 3(b)] the situation is very different. Although the number of the symmetry operations is the same as in the [100] case, the list of operations is different: E, ΘC_{2z}, ΘC_{2b}, C_{2a}, I, $\Theta\sigma_z$, $\Theta\sigma_b$, σ_a. The operations lead to the equivalence of the pairs of atoms: Atom 1 is equivalent to atom 3 and atom 2 is equivalent to atom 4. The atoms from different pairs are not transformed into one another and therefore are not equivalent. The symmetry operations impose the constraint that for each atom $m_x = m_y$, and therefore all moments must remain parallel to the [110] axis, and this ferromagnetic configuration is calculationally stable.

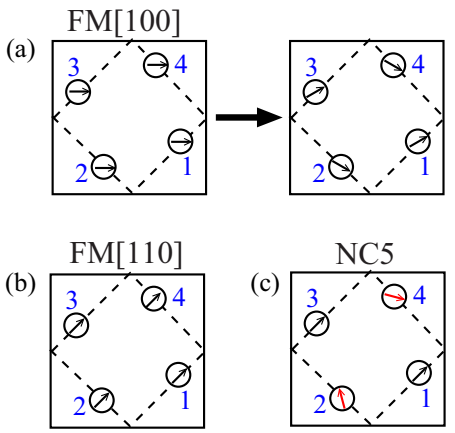

FIG. 3. (a) The ferromagnetic configuration with the U atomic moments parallel to the [100] axis is calculationally unstable and transforms in the noncollinear configuration of the type shown by the arrow and satisfying the constraints $m_{1x} = m_{2x} = m_{3x} = m_{4x}$ and $m_{1y} = -m_{2y} = m_{3y} = -m_{4y}$. (b) The ferromagnetic configuration with the U atomic moments parallel to the [110] axis is calculationally stable. (c) The NC5 configuration with the U_1 and U_3 moments parallel to the [110] axis and the U_2 and U_4 moments canted from the $[1\bar{1}0]$ axis.

IV. FIRST-PRINCIPLES CALCULATIONS FOR VARIOUS MAGNETIC CONFIGURATIONS

A. Nonrelativistic calculations

The calculations confirmed the calculational stability of the FM and NC1-4 configurations predicted by symmetry as well as the equivalence of the four NC states shown in Fig. 1. The atomic moments and the energies of the magnetic configurations are collected in Table II. The energy of the FM state is by 8.2 mRy/UC lower than the energy of the NC1-4 states. Therefore we can conclude that the isotropic Heisenberg exchange is not the origin of the experimental noncollinear ground state structure with orthogonal atomic moments.

Although the NC1-4 configurations are calculationally stabilized by the symmetry constraint, they do not correspond to a local energy minimum. The broken curve in Fig. 4 shows the calculated energies of the magnetic structures obtained from the NC1 structure by the in-plane rotation of the U_1 moment by angles up to 180°. The NC1 structure corresponds to an energy maximum. The energy monotonically decreases with increasing angle and has a minimum at the end of the angular interval where the structure is again stabilized calculationally by the symmetry constraint. More details on the calculations presented in Fig. 4 are given in Sec. VI.

TABLE II. Calculational results for a number of magnetic configurations. The columns give, respectively, the type of magnetic structure, the energy per unit cell (UC), atomic spin, and orbital moments. NC1-5 corresponds to the noncollinear configurations, FM is ferromagnetic configuration, FM[110] is ferromagnetic configuration with all atomic moments parallel to the [110] direction. If all atoms are equivalent only one value of the atomic spin and orbital moments is given. Otherwise, the four values for four U atoms in the unit cell are presented.

mag. struc.	E (mRy/UC)	$m_{sp}(\mu_B)$	$m_{orb}(\mu_B)$
	nonrelativistic calculation		
NC1-4	0	2.159	0
FM	−8.23	2.294	0
	relativistic calculation		
NC1	0	1.931	2.891
NC2	1.48	1.950	2.842
NC3	5.94	1.878	2.457
NC4	7.77	1.891	2.584
FM[110]	1.76	2.025 1.998	2.787 2.572
		2.025 1.998	2.787 2.572
NC5	0.27	1.984 1.969	2.854 2.828
		1.990 1.969	2.790 2.828

B. Relativistic calculations

Also in the relativistic case the calculations confirm the conclusions of the symmetry analysis: The NC1-4 configurations are calculationally stable and inequivalent to each other. In agreement with experiment [12] the energy of the NC1 structure is lower than the energy of the other three structures (see Table II). Note that an earlier calculation [20] for another representative of this class of U compounds, U_2Pd_2Sn [21], also gave the energy of the NC1 structure to be the lowest between four NC1-4 structures. Thus this feature appears to be a stable characteristic of the U_2Pd_2X compounds with complex noncollinear magnetic structures.

We remark that the NC1 state with the lowest energy corresponds to the largest value of the atomic orbital moment that supports the validity of the much discussed correlation between the easy axis direction and the value of the orbital moment (see, e.g., Refs. [14,22,23]).

The FM configuration with the moments parallel to the [110] axis, as predicted, is calculationally stable with inequivalent pairs of atoms: U_1 is equivalent to U_3 and U_2 is equivalent to U_4, but atoms of different pairs are inequivalent to one another. This inequivalence is reflected in somewhat different values of the spin and orbital moments (Table II).

If we slightly deviate the U moments of the FM[110] structure from the [110] direction destroying symmetry constraint the self-consistent calculations result in the magnetic configuration NC5 shown in Fig. 3(c). The orbitals moments of atoms U_2 and U_4 deviate from the $[1\bar{1}0]$ axis by 23.2°. The spin moments of these atoms are almost antiparallel to the orbital moments and deviate from the $[1\bar{1}0]$ axis by 26.9°. Thus the noncollinearity of the two atomic moments is characterized by angle 3.7°. The energy of the NC5 state is only 0.27 mRy/UC higher than the energy of the NC1 state and is considerably lower than the energies of the NC2-4 states. We will come back to the properties of the NC5 state when discussing the in-field calculations and the origin of the metamagnetic transition (Sec. VI).

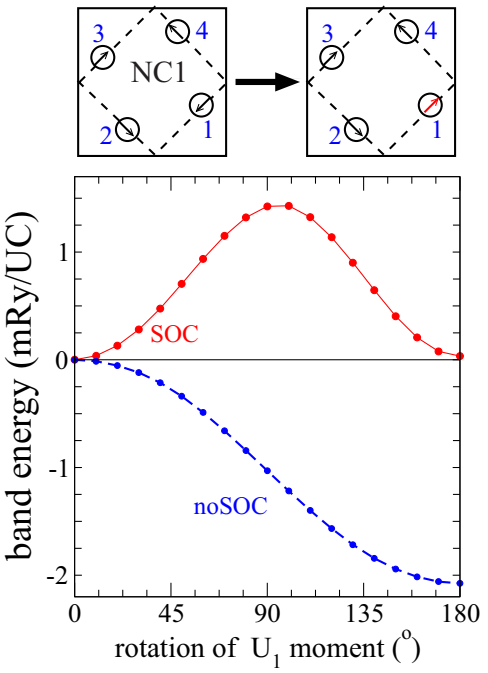

FIG. 4. The band energy of the magnetic structures obtained by the in-plane rotation of the direction of the magnetic moment of the U_1 atom starting with the NC1 structure. The solid two-minima curve is obtained in the relativistic calculations; the broken monotonic curve is obtained with the SOC being neglected. In the upper part of the figure, the unit cells of the magnetic structures corresponding to the end points of the angular interval are depicted.

V. MODEL BILINEAR HAMILTONIAN OF INTERACTING ATOMIC MOMENTS

A. Introduction and symmetry properties

To get insight into the competition of the interactions leading to the physical stability of the NC1 configuration we consider the bilinear Hamiltonian of a general form

$$H = \sum_{IJ} \hat{\boldsymbol{S}}_I A^{IJ} \hat{\boldsymbol{S}}_J^T, \tag{7}$$

where capital letter index $I = (in)$ includes the number of the atom within the unit cell i and the index of the unit cell n, T means matrix transposition, $A^{IJ} \equiv A(in; jm)$ are 3×3 matrices in the coordinate space, and $\hat{\boldsymbol{S}}_I$ is the unit vector in the direction of the Ith atomic moment. The atomic moments are treated as classical vectors. We remark that instead of unit vectors $\hat{\boldsymbol{S}}_I$ one can chose spin or total atomic moments as independent variables. These choices are physically equivalent leading to the numerical modification of the parameters of the Hamiltonian. Our choice of independent variables agrees with the choice used, e.g., in Ref. [24]. The symmetry consideration presented below is invariant with respect to the choice of the independent variables.

It is convenient to split the energy of the interaction between a pair of atoms I and J ($I \neq J$) into two equal parts described by matrices A^{IJ} and A^{JI} that satisfy the relation

$$A^{JI} = A^{IJ\,T}.$$

Matrix A^{IJ} can be written as the sum of the symmetric and antisymmetric parts

$$A^{IJ} = B^{IJ} + C^{IJ}, \tag{8}$$

where

$$B^{IJ} = \tfrac{1}{2}(A^{IJ} + A^{JI}) \quad C^{IJ} = \tfrac{1}{2}(A^{IJ} - A^{JI}). \tag{9}$$

The energy contribution due to the antisymmetric part can be recast as

$$\hat{\boldsymbol{S}}_I C^{IJ} \hat{\boldsymbol{S}}_J^T = \boldsymbol{D}_{IJ} \cdot [\hat{\boldsymbol{S}}_I \times \hat{\boldsymbol{S}}_J] \tag{10}$$

and corresponds to the DMI. The DMI vector $\boldsymbol{D}_{IJ}$ is defined as $\boldsymbol{D}_{IJ} = (C_{xy}^{IJ}, -C_{xz}^{IJ}, C_{yz}^{IJ})$. The symmetric parts B^{IJ} of the matrices supply energy contributions of the isotropic Heisenberg's exchange and magnetic anisotropy.

Symmetry operations of the crystal impose constraints on the elements of the A matrices. The symmetry restriction on matrices A^{IJ} imposed by the symmetry operation $\{\alpha_S|\alpha_R|\boldsymbol{\tau}_\alpha\}$ is given by the expression

$$A(i0; j\boldsymbol{R}_n) = \alpha_S^T A[i_\alpha, 0;\ j_\alpha, \alpha_R \boldsymbol{R}_n + (\boldsymbol{R}_{\alpha j} - \boldsymbol{R}_{\alpha i})]\alpha_S, \tag{11}$$

where the number of the uranium sublattice i_α and lattice vector $\boldsymbol{R}_{\alpha i}$ are defined by

$$\{\alpha_R|\boldsymbol{\tau}_\alpha\}\boldsymbol{a}_i = \boldsymbol{a}_{i_\alpha} + \boldsymbol{R}_{\alpha i}. \tag{12}$$

It is straightforward to show that for the nonrelativistic case the symmetry condition (12) leads to an expected result that the matrices A^{IJ} have a scalar form $J^{IJ}E$ where J^{IJ} is a scalar parameter of the isotropic exchange interaction between atoms I and J and E is the unity matrix. The contributions of the magnetic anisotropy and DMI vanish.

In the relativistic case, the situation is more complex. In general all elements of the A^{IJ} matrix are nonzero. As we have seen [Eqs. (8)–(10)], the antisymmetric part of the matrix corresponds to the DMI. The symmetric part can be represented as a sum of a scalar matrix $J^{IJ}E$ and zero-trace matrix $\overline{B}^{IJ}$. J^{IJ} can be treated as the isotropic Heisenberg exchange parameter; $\overline{B}^{IJ}$ describes anisotropy due to the SOC. Because in this paper we are focusing on the properties of in-plane magnetic structures, below in this section, for the sake of brevity, we will use the 2D form of the vectors and matrices giving only their x and y components. We will start with the properties of the on-site matrices A^{II}. Since the crystallographic positions of all U atoms are equivalent it is sufficient to consider atom U_1 in the unit cell at $n = 0$. The operation $\{C_{2a}|C_{2a}|(\frac{1}{2}, -\frac{1}{2})\}$ transforms atom U_1 into itself. This operation imposes the following symmetry constraint on the elements of the matrix $A(1,0;1,0)$

$$\begin{pmatrix} A_{xx} & A_{xy} \\ A_{yx} & A_{yy} \end{pmatrix} = \begin{pmatrix} A_{yy} & A_{yx} \\ A_{xy} & A_{xx} \end{pmatrix}. \tag{13}$$

Therefore, the on-site matrix $A(1,0;1,0)$ has the symmetric form

$$A(1,0;1,0) = \begin{pmatrix} \alpha & \beta \\ \beta & \alpha \end{pmatrix}. \tag{14}$$

The diagonalization of the matrix gives two eigenvalues

$$\lambda_{1,2} = \alpha \mp \beta$$

that are different if the off-diagonal matrix element β is not zero. We remind that the nonzero off-diagonal element is a consequence of the SOC. The corresponding eigenvectors are $\mathbf{x}_{1,2} = (1, \mp 1)$. Thus, the symmetry consideration shows that the on-site term of the bilinear Hamiltonian gives the local magnetic anisotropy of the U atoms with easy and hard axes parallel to vectors $(1, \mp 1)$. These are the directions of the U moments in the NC1-4 structures. Which of the two axes is the easy one and which is the hard one cannot be established on the basis of symmetry arguments and needs direct first-principles calculations.

Next we consider symmetry properties of the interaction matrix between atom U_1 and the nearest atom U_3 belonging to the unit cell characterized by the lattice vector (1,0) [see Fig. 2(a)]. The account for the symmetry operations with point transformations C_{2z} and C_{2b} transforming atoms U_1 and U_3 into each other (Table I) leads to the form of the matrix $A[1,0;3,(1,0)]$ that coincides with the form of the matrix $A(1,0;1,0)$ given above in Eq. (14). This matrix is symmetric and therefore no DMI interaction can appear between atoms U_1 and U_3. The directions of the easy and hard axes of this interaction are again given by the vectors $(1, \mp 1)$.

Considering the interaction between atom U_1 and four neighboring atoms of the type U_2 and U_4 (Fig. 2), we get the following properties of the interaction matrices. Matrix $A(1,0;2,0)$ has the form

$$A(1,0;2,0) = \begin{pmatrix} \delta & \gamma \\ -\gamma & \delta \end{pmatrix}, \tag{15}$$

where γ contributes to the antisymmetric part of the matrix and determines the strength of the DMI interaction between two atomic moments. Knowing the form of $A(1,0;2,0)$, the symmetry determines uniquely the form of the other three matrices $A[1,0;2,(1,0)] = A(1,0;2,0)$ and $A(1,0;4,0) = A[1,0;4,(0,-1)] = A(1,0;2,0)^T$.

Then the energy of the interaction of the moment of atom U_1 with the four neighboring U_2 and U_4 atoms is given by

$$E_{1,\{2,4\}} = 2\boldsymbol{S}_1 \begin{pmatrix} \delta & \gamma \\ -\gamma & \delta \end{pmatrix} \boldsymbol{S}_2^T + 2\boldsymbol{S}_1 \begin{pmatrix} \delta & -\gamma \\ \gamma & \delta \end{pmatrix} \boldsymbol{S}_4^T. \tag{16}$$

If $\boldsymbol{S}_2 = -\boldsymbol{S}_4$ as in the case of our NC1-4 magnetic structures, the energy takes the form

$$E = 4\boldsymbol{S}_1 \begin{pmatrix} 0 & \gamma \\ -\gamma & 0 \end{pmatrix} \boldsymbol{S}_2^T \tag{17}$$

and only the DMI remains operative. On the other hand, if $\boldsymbol{S}_2 = \boldsymbol{S}_4$ we have

$$E = 4\boldsymbol{S}_1 \begin{pmatrix} \alpha & 0 \\ 0 & \alpha \end{pmatrix} \boldsymbol{S}_2^T \tag{18}$$

and only the contribution of the isotropic Heisenberg exchange remains.

In summary, the symmetry analysis of the properties of the interaction matrices A^{IJ} shows that both local anisotropy of the U atoms and the DMI between atoms U_1,U_3 and atoms U_2,U_4 can be responsible for the peculiar ground state of the U_2Pd_2In. To reveal relative strength of different interactions we proceed further with the consideration of the first-principles relativistic calculations.

B. Analysis of the interatomic interactions on the basis of first-principles calculations

First, we emphasize the large difference in the relative energies of different magnetic configurations obtained in nonrelativistic and relativistic calculations. For instance, in the nonrelativistic calculation the FM structure is 8.23 mRy/UC lower than the NC1 structure, whereas in the relativistic calculation FM[110] structure is 1.76 mRy/UC higher. Simultaneously, the equal nonrelativistic energies of the NC1-4 structures are spread over the interval of about 8 mRy/UC in the relativistic case.

To illustrate the origin of these differences we plot in Fig. 5 the uranium density of states (DOS) of various magnetic configurations calculated both nonrelativistically and relativistically. There are strong changes in the characteristic width of the DOS between nonrelativistic and relativistic calculations. Also, the change of the magnetic structure leads to substantial reconstruction of the DOS. The change of the total energy of the system reflects, in an integrated form, the changes of the energies of individual electronic states. The complexity of the dependence of the electronic structure on both the magnetic configuration and the SOC indicates the limitations of the description of the underlying physics in terms of several parameters of effective interatomic interactions. As discussed below, these limitations reveal themselves in the form of an inability to quantitatively describe the results of first-principles calculations with a simple bilinear Hamiltonian of interacting atomic moments. However, the examination of the results of first-principles calculations establishes different energy ranges of different interactions that is crucial for our analysis of the ground state and metamagnetic transition.

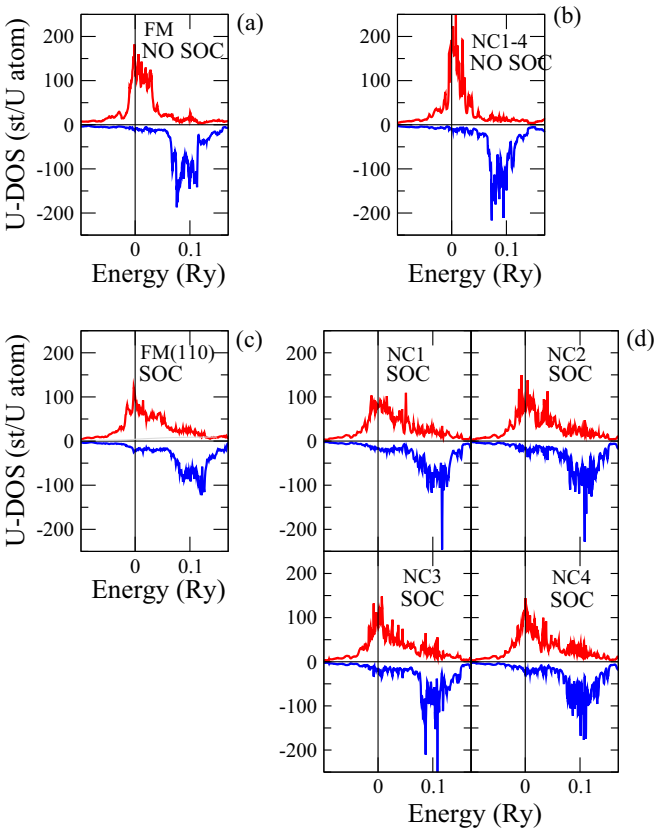

FIG. 5. The calculated U-DOS for various magnetic structures. (a) Ferromagnetic structure, nonrelativistic calculation; (b) noncollinear NC1-NC4 structures, nonrelativistic calculation; (c) ferromagnetic FM(110) structure, relativistic calculation; (d) noncollinear NC1-NC4 structures, relativistic calculation. The curves with positive values correspond to the spin-up DOS; the curves with negative values correspond to the spin-down DOS. The spin projections are shown with respect to the local atomic spin axes. The zero energy corresponds to the Fermi energy.

If we keep relative orientation of the atomic moments of the NC1 structure unchanged and rotate them rigidly about the z axis, the NC1 state transforms into NC4. This transformation does not change the contributions of the DMI and isotropic exchange to the energy calculated with the bilinear model Hamiltonian. It, however, changes the energy due to the local magnetic anisotropy of the atoms. Similarly, the transformation of the NC2 structure into NC3 corresponds to the change of the magnetic anisotropy energy (MAE) and preserves the exchange and DMI energy of the bilinear model. The energies of the intermediate states can be obtained by the relativistic constraint calculations and are shown in Fig. 6. They have the form of monotonic curves with zero derivatives at the ends of the angular interval. The monotonic behavior of the curves corresponds to the form expected on the basis of the bilinear Hamiltonian. However,

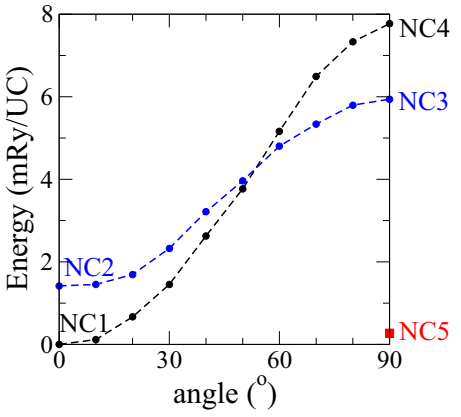

FIG. 6. The energies of the magnetic configurations obtained from the NC1 (black curve) and NC2 (blue curve) structures by rigid rotation of all atomic moments by an angle given at the abscissa axis. The end point of the black (blue) curve corresponds to the NC4 (NC3) structure. The energies are counted from the energy of the NC1 state and given in mRy per unit cell. The red square at the right ordinate axis gives the energy of the NC5 state. The figure shows the results of the relativistic calculations. In the nonrelativistic case the energies of the NC1-4 structures as well as of all intermediate structures shown in the figure are exactly equal to each other.

the energy differences $\delta_{41} = E_{NC4} - E_{NC1} = 7.77$ mRy/UC and $\delta_{32} = E_{NC3} - E_{NC2} = 4.96$ mRy/UC are not equal to each other, in contrast to what is expected from the bilinear Hamiltonian. This shows that the model bilinear Hamiltonian with a fixed set of parameters of two-atom interactions does not provide a quantitative description of the energetics of the magnetic configurations of the system. It, however, can be used to estimate the scale of different interactions.

The energy differences $\delta_{21} = E_{NC2} - E_{NC1} = 1.48$ mRy/UC and $\delta_{34} = E_{NC3} - E_{NC4} = 1.83$ mRy/UC must be assigned to the DMI interaction. The DMI energies, although again different, are much closer to each other than to both MAE energies and much smaller than the MAE energies.

To estimate the strength of the interatomic exchange interaction between atoms U_1 and U_3 we reverse the direction of the atomic moment of the U_3 atoms. If we do this for the ground-state structure NC1 we obtain an increase in the total energy of 0.47 mRy/UC. The same procedure for the NC2 structure gives a decrease of the total energy of 0.35 mRy/UC. In the nonrelativistic calculation the energy decreases by 3.09 mRy/UC for all four structures NC1-4. These calculations show that the account for the SOC changes the values of the effective exchange interactions very strongly. The relativistic estimations with the use of different magnetic configurations give somewhat different values showing again that there is no universal description of all magnetic structures with the simple effective bilinear Hamiltonian discussed in Sec. V A. However, the orders of magnitude of different interactions are different. These results show that the effect of the local magnetic anisotropy provides the largest energy scale in the considered energetic balance.

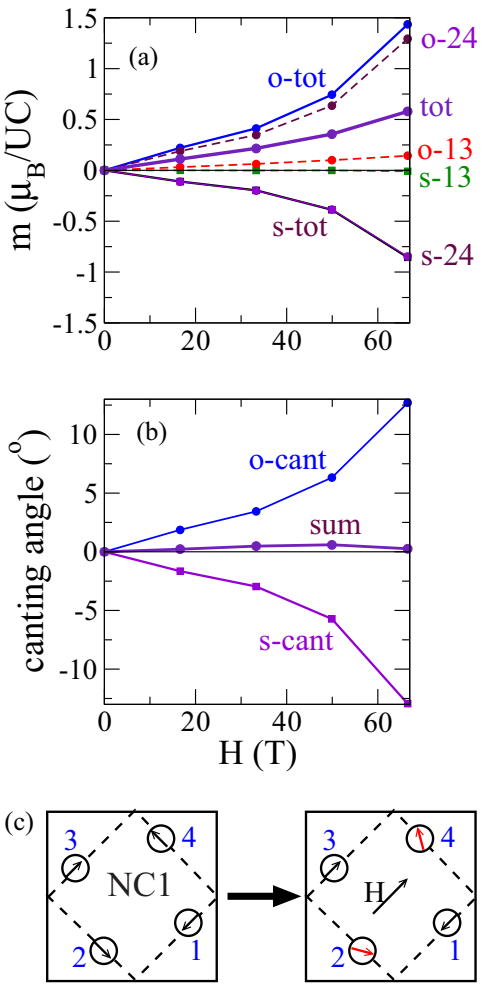

FIG. 7. Calculated induced moments (a) and canting angles (b) as a function of the value of the magnetic field acting on the NC1 structure and applied parallel to the [110] direction [see panel (c)]. The values of the magnetization are given in the units of μ_B per unit cell (UC). The lines marked with o-tot and s-tot give the orbital and spin contributions to the total magnetization marked with tot. The lines marked with o-13 and s-13 give the orbital and spin contributions of atoms U_1 and U_3. Respectively, the lines marked with o-24 and s-24 give the orbital and spin contributions of atoms U_2 and U_4. o-cant and s-cant in the (b) panel give the values of the canting angles of the orbital and spin moments of the U_2 and U_4 atoms. The positive (negative) value of the canting means the deviation of the moments towards (opposite to) the direction of the magnetic field. The sum of the o-cant and s-cant dependences gives the angle of the deviation of the atomic spin and orbital moments from the antiparallel directions.

VI. CALCULATIONS OF U_2Pd_2In IN APPLIED MAGNETIC FIELD

The experimental observation of the metamagnetic phase transition in the applied magnetic field motivated us to perform DFT calculation of U_2Pd_2In in external magnetic field. The magnetic field enters the calculations through the Zeeman term with the field acting on both spin and orbital magnetic moments. The field was applied to the ground-state NC1 structure and directed parallel to the in-plane [110] axis.

Experiment at 4.2 K shows [12] that with increasing strength of the applied field the induced magnetization increases, approximately linearly, up to the field of about 25 T. At this field the magnetization jumps discontinuously signifying the presence of the first-order phase transition. With further increasing field up to 30 T the magnetization continues to increase with the slope comparable to those before the transition.

The presence of external magnetic field decreases the symmetry of the problem destroying the invariance of the system with respect to the C_{4z} operation. As a result, the symmetry constraint responsible for the calculational stability of the NC1 structure is disturbed. The remaining symmetry operations keep the moments of U_1 and U_3 collinear to the [110] axis. The atoms U_1 and U_3 become, however, nonequivalent to each other and to atoms U_2 and U_4. On the other hand, the U_2 and U_4 remain equivalent but do not preserve the directions collinear to the $[1\bar{1}0]$ axis and become canted, by equal angles, towards the [110] axis [see Fig. 7(c)].

The contributions to the induced magnetic moment come from the inequivalence of atoms U_1 and U_3 and from the canting of the moments of atoms U_2 and U_4. One can expect that the moment of atom U_3 that is parallel to the field will increase whereas the moment of atom U_1 that is antiparallel to the field will decrease. The canting of the moments of the atoms U_2 and U_4 should also give the contribution parallel to the field. There is however a subtle aspect of the problem related

to the properties of the spin and orbital contributions to the induced moment. Through the Zeeman term, the applied field tends to make contributions of both spin and orbital moments to the induced magnetization to be parallel to the field. This means that, for example, the orbital moment of atom U_3 should show the trend to increase and the spin moment to decrease. However, the SOC connects the spin and orbital moments, and increase (decrease) of the magnitude of one of them produces the trend to the increase (decrease) of the magnitude of the other. Therefore, we have a competition of two different trends originating from the external magnetic field and SOC.

Also in the case of canted moments of atoms U_2 and U_4 we expect the competition of the trends: The magnetic field tends to move both spin and orbital moments towards the [110] axis disturbing antiparallelity of the two atomic moments. On the other hand, on-site SOC tends to keep these moments antiparallel.

In Fig. 7(a) we show the results of the calculations for the applied magnetic field up to 67 T. The lines marked with o-tot and s-tot give the orbital and spin contributions to the total magnetization marked with tot in the figure. We see that the main contribution to the induced magnetization comes from the orbital moment. The spin contribution is opposite to the field revealing a stronger effect of the SOC and third Hund's rule compared to the direct influence of the applied field.

In Fig. 7(a), we also show the partial contributions of atoms U_1 and U_3 (o-13 and s-13 for, respectively, spin and orbit contributions) and atoms U_2 and U_4 (o-24 and s-24 contributions). The moments of the atoms U_1 and U_3 collinear to the applied field give negligibly small spin contribution and rather small positive orbital contribution. The contributions coming from the canting of the moments of atoms U_2 and U_4 are considerably larger. The canting angles of the orbital and spin moments are shown in Fig. 7(b). The sign of the angle is positive for the canting towards the direction of the field and negative for the canting in the opposite direction. The negative sign of the spin canting shows that the effect of the SOC and third Hund's rule is stronger than the direct influence of the field. The line marked as sum in Fig. 7(b) shows the deviation of the spin and orbital moments of atoms U_2 and U_4 from 180°. This deviation, although clearly detectable, is rather small. So, the spin and orbital atomic moments remain roughly antiparallel.

The discontinuous transition to a metamagnetic state with a large ferromagnetic component observed experimentally is not obtained in this calculation. Above in Sec. IV B we discussed the NC5 state of the system that, first, possesses large net magnetization and, second, has an energy close to the energy of the ground state NC1 structure. By symmetry, the NC5 structure is compatible with the symmetry of the NC1 structure subjected to the magnetic field in the [110] direction. Apparently, our in-field calculation should reproduce the metamagnetic NC1 to NC5 transition. However, this transition was not obtained and the system remained close to the NC1 state. The following calculation helps to understand the origin of the metamagnetic transition and to explain the absence of the transition in the in-field calculation. We performed constrained calculation for the magnetic configurations obtained from the NC1 structure by the in-plane rotation of the U_1 moment by the angle in the interval between 0 and 180°. The final structure corresponding to the reversal of the direction of the U_1 moment is similar to the NC5 structure but without the canting of the U_2 and U_4 moments from the $[1\bar{1}0]$ axis. In this calculation we applied magnetic force theorem [25] and evaluated the change of the band energy.

We obtained that the energy of the system first increases strongly and then decreases again to the value close to that of the ground state NC1 structure (see Fig. 4). The form of the curve can be interpreted on the basis of our results for the strengths of different contributions to the energy of magnetic states. The energy barrier between two minima (Fig. 4) corresponds to the increased energy of the U_1 moment when its direction passes through the direction of the hard magnetization and, therefore, has its origin in the local magnetic anisotropy of the U atoms. The relativistic origin of the energy barrier is confirmed by the calculations for the same set of magnetic configurations performed with the SOC being neglected. In this case we obtain a monotonic decrease of the energy in strong contrast with relativistic calculation (Fig. 4).

The two-minima energy curve suggests the following interpretation of the metamagnetic phase transition. The magnetic configuration with reversed U_1 moment has the energy that is only slightly higher than the energy of the ground state. Since, in contrast to the NC1 structure, this state has a large net moment the applied magnetic field decreases the energy of the state below the energy of the NC1 state that results in the metamagnetic transition. Our DFT calculations with magnetic field applied to the NC1 configuration do not describe this transition. This deficiency of the DFT calculation should be expected. The first-order phase transition between two states separated by an energy barrier is a complex physical process where fluctuations not accounted for in our DFT calculations play a decisive role. For example, the fluctuations breaking translational symmetry of the magnetic structures are not considered in our calculations. We also expect that the magnetic states with atomic moments deviating from the xy plane and quantum-mechanical tunneling of atomic moments

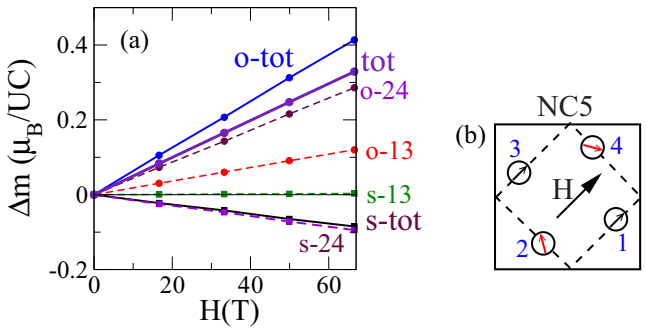

FIG. 8. Calculated induced moments (a) as a function of the value of the magnetic field acting on the NC5 structure and applied parallel to the [110] direction [see panel (b)]. The values of the magnetization are given in the units of μ_B per unit cell. The lines marked with o-tot and s-tot give the orbital and spin contributions to the total magnetization marked with tot. The lines marked with o-13 and s-13 give the orbital and spin contributions of atoms U_1 and U_3. Respectively, the lines marked with o-24 and s-24 give the orbital and spin contributions of atoms U_2 and U_4.

play an important role in the overcoming of the barrier. All these effects are not included in the present study.

It is of interest to look also at the influence of the magnetic field on the metamagnetic state. The in-field calculation for the NC5 configuration shows (see Fig. 8) that the properties of the field response of the metamagnetic NC5 state are in many respects similar to the properties of the induced magnetization for the ground-state NC1 structure (Fig. 7). The leading contribution to the induced total moment comes from the orbital moment. The contribution of the spin moment is negative showing again that the mechanism of the third Hund's rule is stronger than the direct influence of the field. Again, the contribution to the induced moment due to the canting of the moments of atoms U_2 and U_4 is stronger than the contribution due to the varied values of the U_1 and U_3 moments collinear to the field. Comparable magnetic response of the ground and metamagnetic states to the applied field is in agreement with the in-field measurements [12].

VII. CONCLUSIONS

U_2Pd_2In is the material where the elements of the geometrical frustration coexist with strong SOC. The ground state of the system is a noncollinear planar magnetic structure with orthogonal atomic magnetic moments. There are three possible physical mechanisms that can lead to this nontrivial magnetic structure: frustrated isotropic exchange interaction, DMI, and magnetic anisotropy. Our first-principles calculations show that in the case where the SOC is neglected, and therefore the DMI and magnetic anisotropy are absent, the ground state structure is the collinear ferromagnetic one. The leading contribution to the stabilization of the magnetically compensated configuration of orthogonal atomic moments is provided by the local magnetic anisotropy of the U moments. A weaker DMI leads to the lifting of the degeneracy between the magnetic states with different local chirality. The established hierarchy of the interactions allows us to explain the metamagnetic phase transition in the in-plane external magnetic field. The analysis of the noncollinearity of the spin and orbital moments of the same U atom appearing in the applied external field show that the trend to the antiparallel orientation of the two atomic moments following from the third Hund's rule is much stronger than the trend to the parallel orientation of the moments due to the applied external magnetic field.

ACKNOWLEDGMENTS

The author gratefully acknowledges discussions with Karel Prokeš.

[1] R. Moessner and A. P. Ramirez, Phys. Today **59**, 24 (2006).
[2] Hiroshi Takatsu, Gwilherm Nenert, Hiroaki Kadowaki, Hideki Yoshizawa, Mechthild Enderle, Shingo Yonezawa, Yoshiteru Maeno, Jungeun Kim, Naruki Tsuji, Masaki Takata, Yang Zhao, Mark Green, and Collin Broholm, Phys. Rev. B **89**, 104408 (2014).
[3] J. D. M. Champion, A. S. Wills, T. Fennell, S. T. Bramwell, J. S. Gardner, and M. A. Green, Phys. Rev. B **64**, 140407(R) (2001).
[4] Z. L. Dun, J. Trinh, K. Li, M. Lee, K. W. Chen, R. Baumbach, Y. F. Hu, Y. X. Wang, E. S. Choi, B. S. Shastry, A. P. Ramirez, and H. D. Zhou, Phys. Rev. Lett. **116**, 157201 (2016).
[5] I. E. Dzyaloshinskii, J. Phys. Chem. Solids **4**, 241 (1958).
[6] T. Moriya, Phys. Rev. **120**, 91 (1960).
[7] P. Bak and M. H. Jensen, J. Phys. C **13**, L881 (1980).
[8] S. Mühlbauer, B. Binz, F. Jonietz, C. Pfleiderer, A. Rosch, A. Neubauer, R. Georgii, and P. Böni, Science **323**, 915 (2009).
[9] Stefan Heinze, Kirsten von Bergmann, Matthias Menzel, Jens Brede, Andre Kubetzka, Roland Wiesendanger, Gustav Bihlmayer, and Stefan Blügel, Nat. Phys. **7**, 713 (2011).
[10] M. Bode, M. Heide, K. von Bergmann, P. Ferriani, S. Heinze, G. Bihlmayer, A. Kubetzka, O. Pietzsch, S. Blügel, and R. Wiesendanger, Nature (London) **447**, 190 (2007).
[11] L. M. Sandratskii and G. H. Lander, Phys. Rev. B **63**, 134436 (2001).
[12] K. Prokeš, H. Nakotte, M. I. Bartashevich, M. Doerr, and V. Sechovsky, Phys. Rev. B **68**, 014405 (2003).
[13] L. M. Sandratskii, Adv. Phys. **47**, 91 (1998).
[14] L. M. Sandratskii, Phys. Rev. B **88**, 064415 (2013).
[15] Anders Hjelm and Jean-Louis Calais, Phys. Rev. B **48**, 8592 (1993).
[16] L. M. Sandratskii, Phys. Rev. B **64**, 134402 (2001).
[17] B. S. Shastry and B. Sutherland, Physica B+C **108**, 1069 (1981).
[18] Alexei Grechnev, Phys. Rev. B **87**, 144419 (2013).
[19] M. S. Kim, M. C. Bennett, and M. C. Aronson, Phys. Rev. B **77**, 144425 (2008).
[20] L. M. Sandratskii and J. Kübler, Phys. Rev. Lett. **75**, 946 (1995).
[21] A. Purwanto, R. A. Robinson, L. Havela, V. Sechovsky, P. Svoboda, H. Nakotte, K. Prokeš, F. R. de Boer, A. Seret, J. M. Winand, J. Rebizant, and J. C. Spirlet, Phys. Rev. B **50**, 6792 (1994).
[22] P. Bruno, Phys. Rev. B **52**, 411 (1995).
[23] L. M. Sandratskii, Phys. Rev. B **92**, 134414 (2015).
[24] Bernd Zimmermann, Marcus Heide, Gustav Bihlmayer, and Stefan Blügel, Phys. Rev. B **90**, 115427 (2014).
[25] A. I. Liechtenstein, M. I. Katsnelson, V. P. Antropov, and V. A. Gubanov, J. Magn. Magn. Mater. **67**, 65 (1987).